P-Rex1 is required for efficient melanoblast migration and melanoma metastasis

Colin R. Lindsay[1*], Samuel Lawn[1*], Andrew D. Campbell[1*], William J. Faller[1], Florian Rambow[2], Richard L. Mort[3], Paul Timpson[1], Ang Li[1], Patrizia Cammareri[1], Rachel A. Ridgway[1], Jennifer P. Morton[1], Brendan Doyle[1], Shauna Hegarty[4], Mairin Rafferty[5], Ian G. Murphy[6], Enda W. McDermott[6], Kieran Sheahan[6], Katherine Pedone[7], Alexander J. Finn[7], Pamela A. Groben[7], Nancy E. Thomas[7], Honglin Hao[7], Craig Carson[7], Jim C Norman[1], Laura M Machesky[1], William M. Gallagher[5], Ian J. Jackson[3], Leon Van Kempen[8], Friedrich Beermann[9], Channing Der[7], Lionel Larue[2], Heidi C. Welch[10], Brad W. Ozanne[1], and Owen J. Sansom[1#]

Supplementary Material

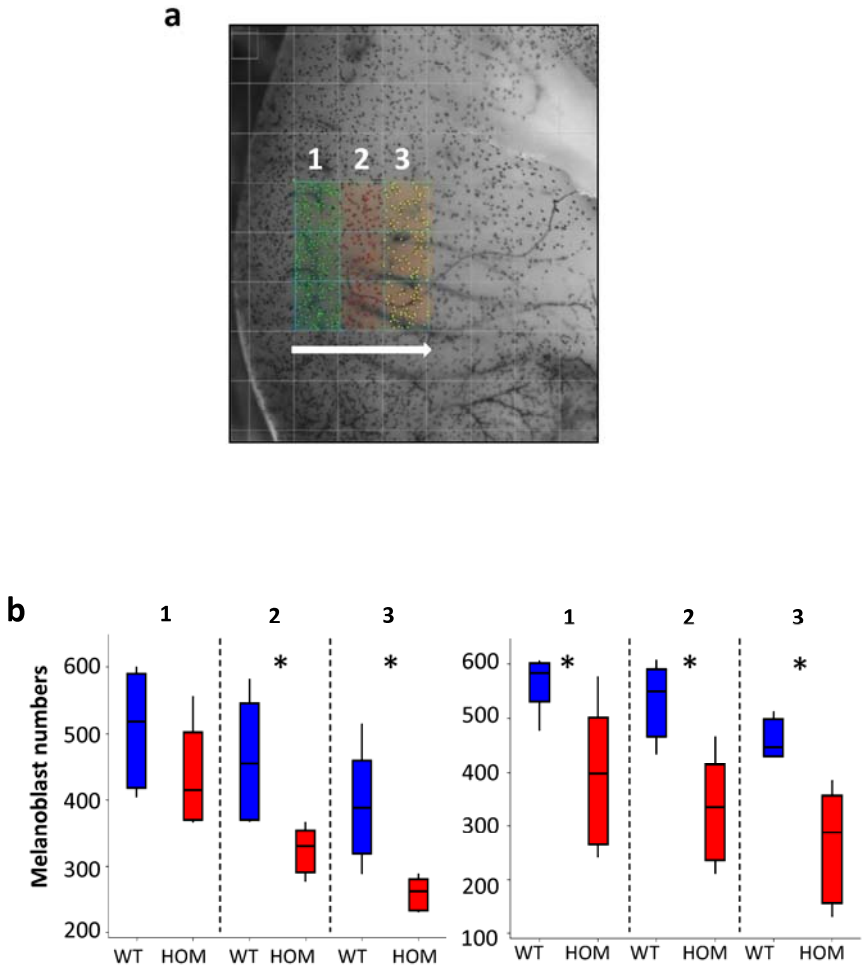

Supplementary Figure S1. P-Rex1$^{-/-}$ mice have an embryological defect in melanoblast migration at E13.5. **(a)** Schematic picture detailing method for quantification of melanoblast cell migration between genotypes at E13.5. Levels 1 to 3 across torso of each embryo represent areas of 500µm x 1500µm. Melanoblasts were counted at each level and their numbers compared between genotypes (**b)** Comparison of melanoblast migration between P-Rex1$^{+/+}$ (blue bars) and P-Rex1$^{-/-}$ (red bars) mice along torso in X-gal stained embryos at E13.5. Left panel represents Nras$^{+/+}$ embryos (*p=0.016/0.021 at levels 2/3, Mann-Whitney test; n=5), right panel represents Nras$^{Q61K/°}$ embryos (*p=0.021/0.021/0.012 at levels 1/2/3, Mann-Whitney test; n=5) (Box and whiskers plots: boxes represent 25th-75th percentiles of given value, lines represent median values).

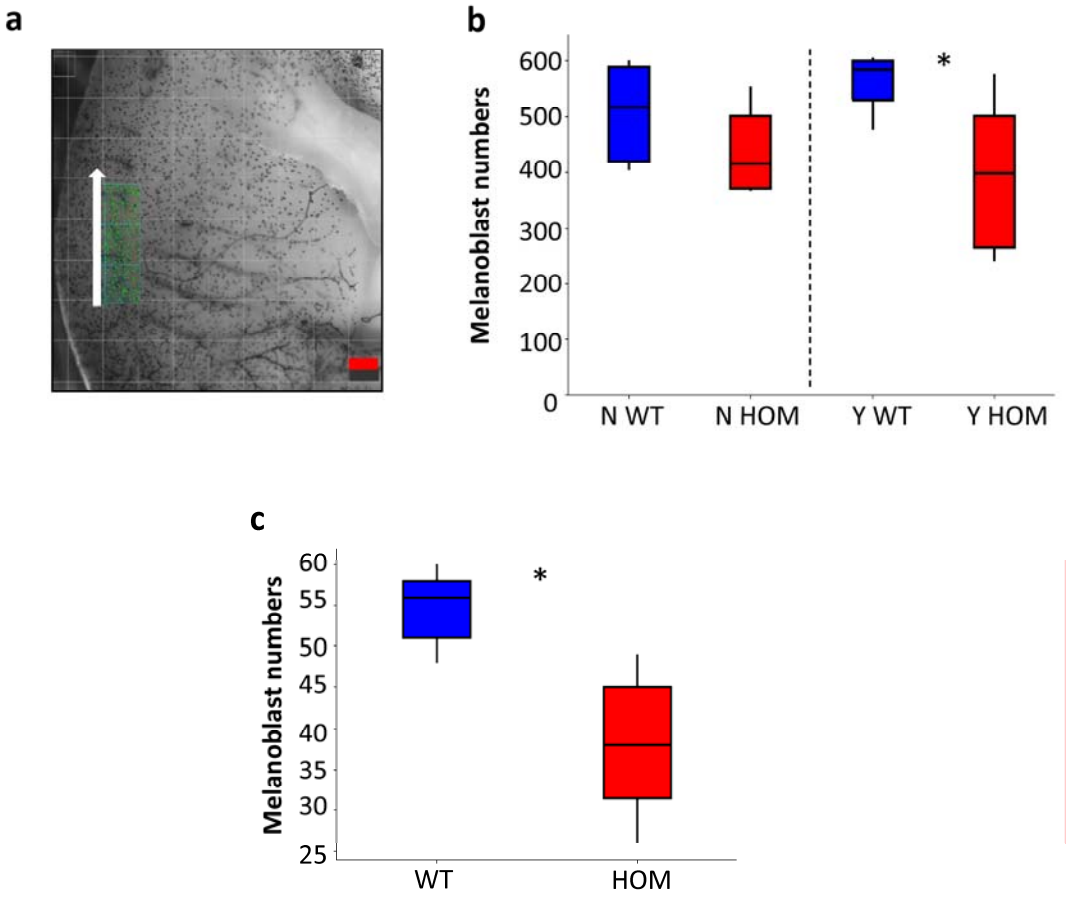

Supplementary Figure S2. Tyr::Nras$^{Q61K/°}$; P-Rex1$^{-/-}$ embryos have a reduction in melanoblast cell numbers **(a)** Schematic pictures detailing method for quantification of melanoblasts at E13.5. Areas represented 500µm x 1500µm. Melanoblasts were counted and their numbers compared between genotypes. **(b)** Comparison of E13.5 melanoblast numbers between P-Rex1$^{+/+}$ (N WT, blue bars) and P-Rex1$^{-/-}$ (N HOM, red bars) mice (left hand panel), and also between Tyr::Nras$^{Q61K/°}$; P-Rex1$^{+/+}$ (Y WT, blue bars) and Tyr::Nras$^{Q61K/°}$; P-Rex1$^{-/-}$ (Y HOM, red bars) mice (right hand panel) (*p =0.02, Mann-Whitney test; n=5) (Box and whiskers plots: boxes represent 25th-75th percentiles of given value, lines represent median values). **(c)** Comparison of E15.5 melanoblast numbers between P-Rex1$^{+/+}$ (WT, blue bars) and P-Rex1$^{-/-}$ (HOM, red bars) mice using live *ex vivo* timelapse (*p =0.007, Mann-Whitney test; n=5).

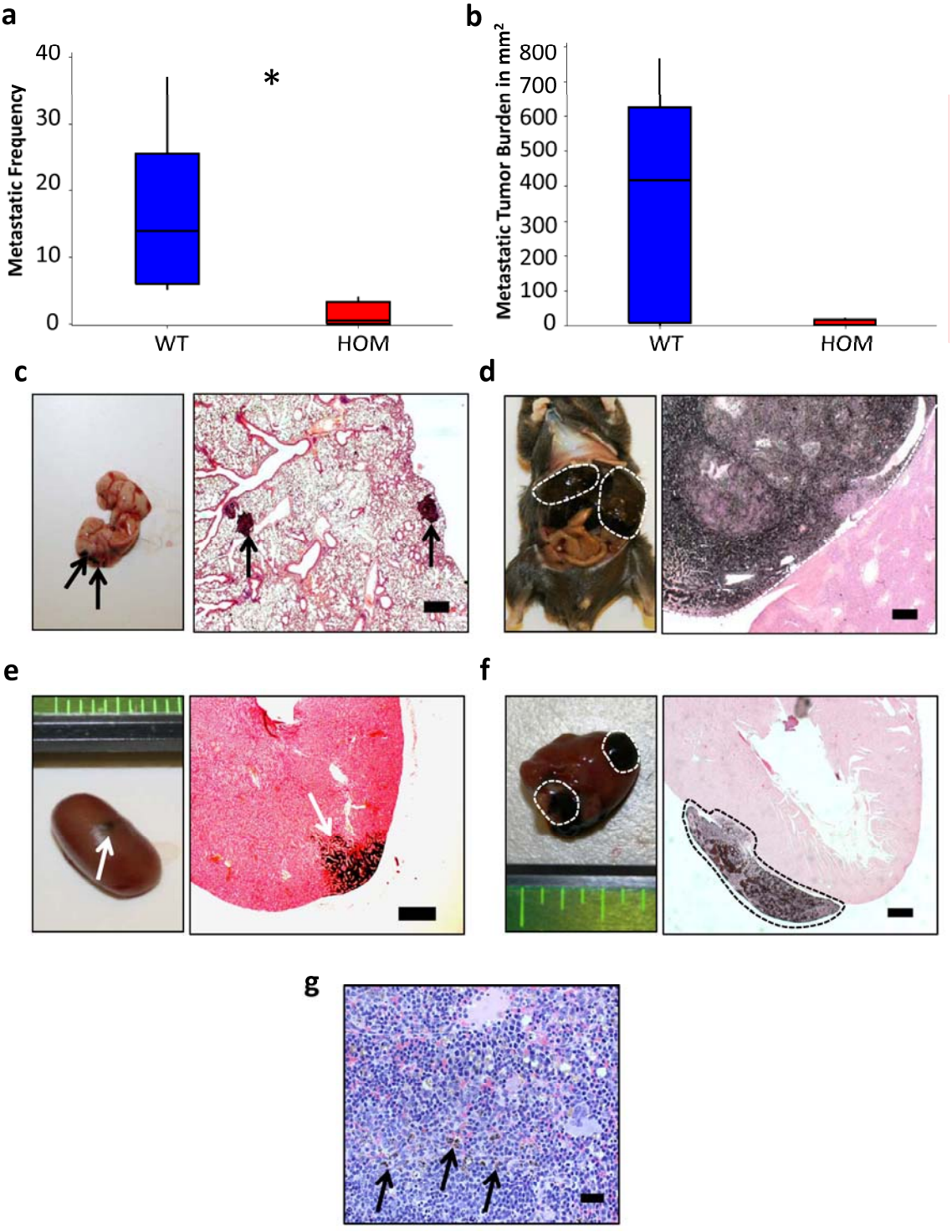
a
Metastatic Frequency
40
30
20
10
0
*
WT
HOM
b
Metastatic Tumor Burden in mm²
800
700
600
500
400
300
200
100
0
WT
HOM
c
d
e
f
g

Supplementary Figure S3. Endogenous P-Rex1 facilitates metastatic frequency, tumor burden and organ spread following the intravasation step **(a)** Quantification of metastases observed in BL6 mice TV-treated with melanocytes derived from early pup skin of either *Tyr::Nras$^{Q61K/°}$; INK4a$^{-/-}$; P-Rex1$^{-/-}$* mice (HOM, red bar) or *Tyr::Nras$^{Q61K/°}$; INK4a$^{-/-}$; P-Rex$^{+/+}$* mice (WT, blue bar) (*p=0.02, Mann-Whitney test; n=5) (Box and whiskers plots: boxes represent 25th-75th percentiles of given value, lines represent median values) **(b)** Quantification of metastatic tumor burden observed in the same BL6 TV-treated mice as described in (a) (p=0.087, Mann-Whitney test; n=5) (Box and whiskers plots: boxes represent 25th-75th percentiles of given value, lines represent median values) **(c) – (f)** Metastatic melanomas affecting lungs (c, black arrows), liver (d, white interrupted line), kidney (e, white arrow), and heart (f, interrupted line) of BL6 mice TV-treated with *Tyr::Nras$^{Q61K/°}$; INK4a$^{-/-}$; P-Rex$^{+/+}$* cells; accompanying photomicrographs (H&E, scale=500µm) **(g)** photomicrograph of micrometastases observed in spleen of BL6 mice TV-treated with *Tyr::Nras$^{Q61K/°}$; INK4a$^{-/-}$; P-Rex$^{+/+}$* cells (H&E, scale=30µm).

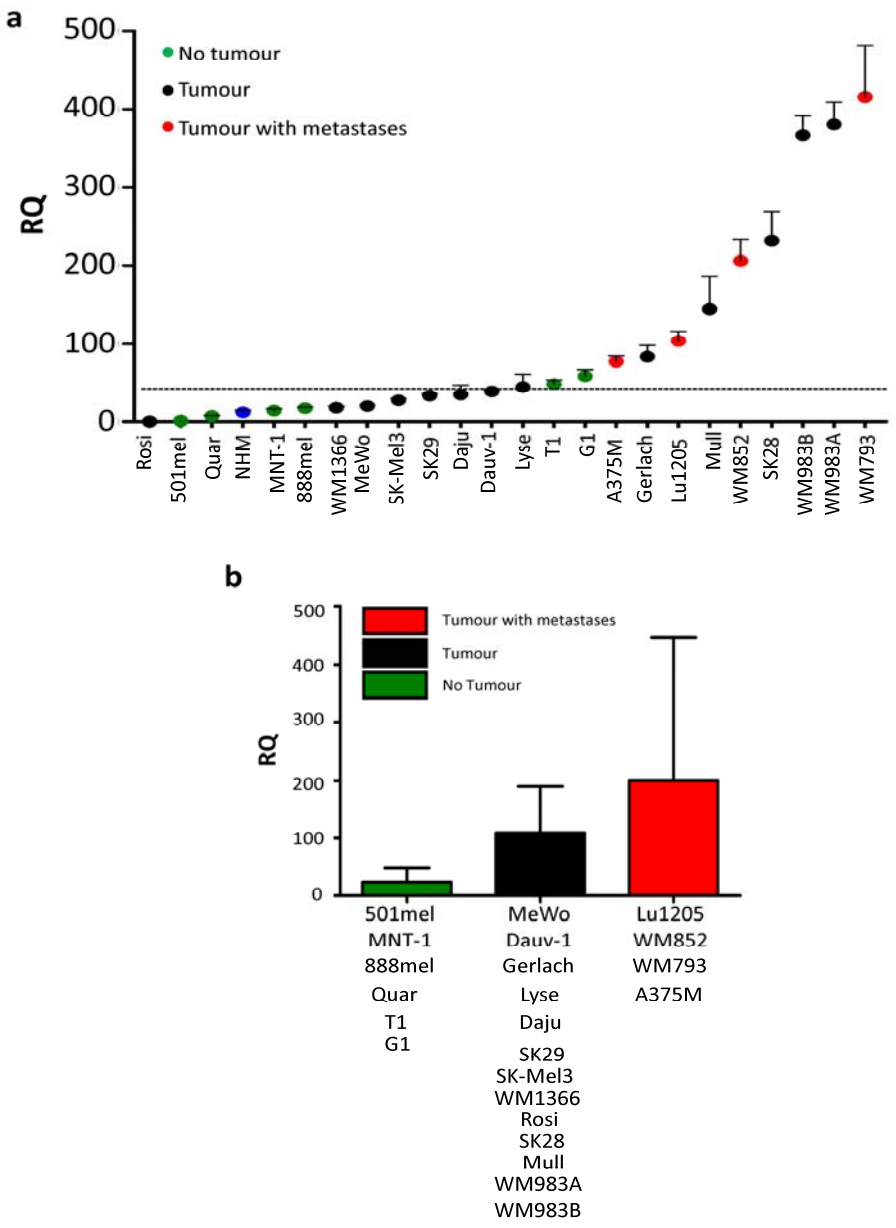

Supplementary Figure S4. High P-Rex1 is sensitive for the development of metastases in immuno-deficient mice. **(a)** Individual value plot from RT-PCR showing P-Rex1 mRNA levels in melanoma-derived cell lines correlate with their propensity to develop metastases in immuno-deficient mice. Interrupted line represents median P-Rex1 value. RQ = relative quantity. NHM = normal human melanocytes. Error bars represent the standard deviation of the triplicate measurement. **(b)** Average RQ values of cell lines in each group. Abbreviations and error bars as described above.

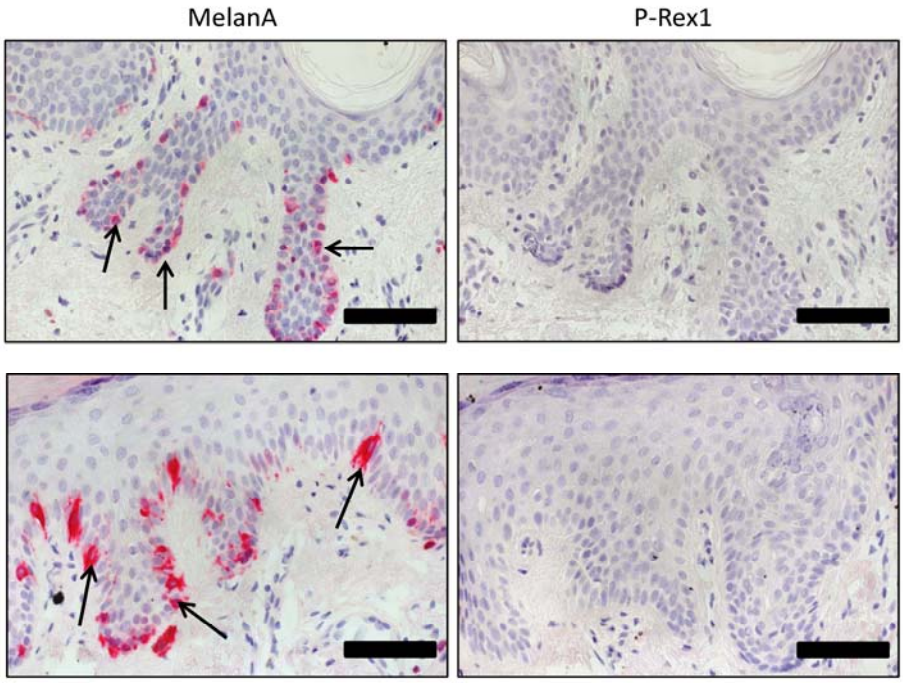

Supplementary Figure S5. P-Rex1 is not detectable in melanocytes by immunohistochemistry. Photomicrographs of human melanocytes (black arrows) of normal skin (serial sections from 2 separate patients) immunohistochemically labelled against P-Rex1 or the melanocyte marker melanA. Similar staining of normal skin from a third patient is seen as part of Figure 4b. Scale bars = 90µm.

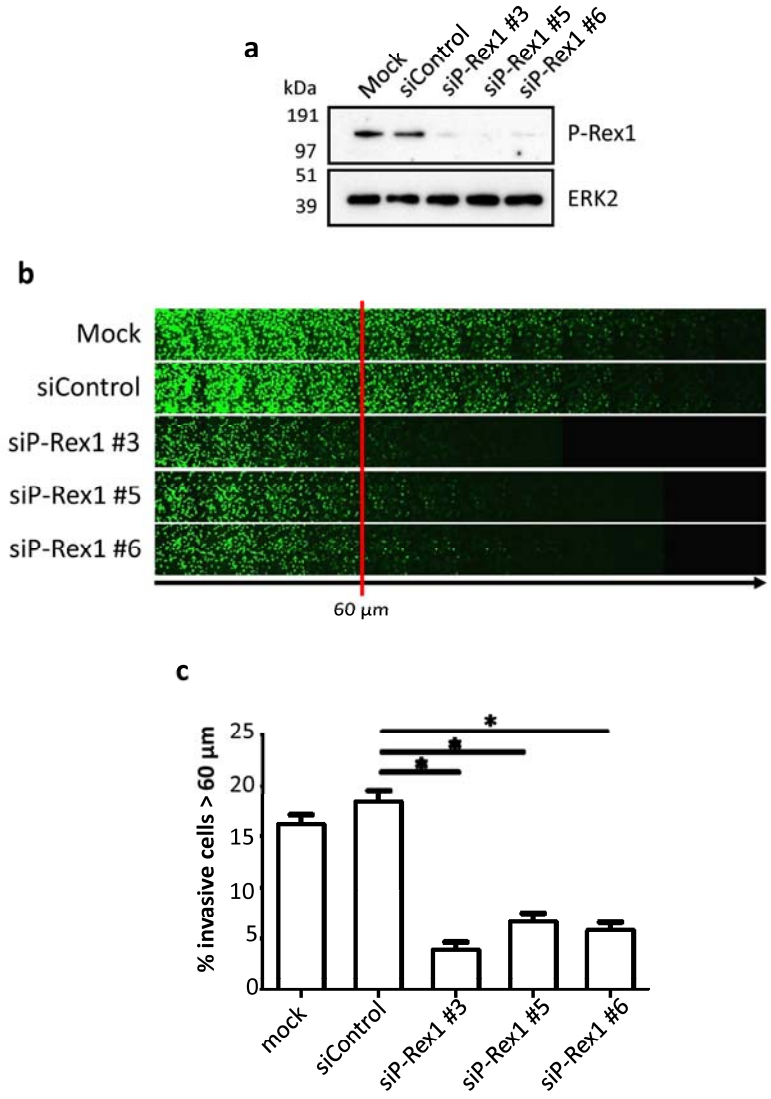

Supplementary Figure S6. Endogenous P-Rex1 enhances invasion in human melanoma **(a)** Silencing P-Rex1 by siRNA as shown by Western blot analysis. A mock transfection and scramble siRNA were used as controls. **(b)** Comparison of representative matrigel invasion assays of WM793 human melanoma cell lines treated with control or P-Rex1 specific siRNA oligonucleotides. **(c)** Quantification of cells invading beyond 60µm in matrigel invasion assays of WM793 human melanoma cell lines treated with control ('siControl') vs P-Rex1 ('siP-Rex1') specific siRNA oligonucleotides. (*p=0.0028, Mann-Whitney test; n=3) (Box and whiskers plots: boxes represent 25^{th}-75^{th} percentiles of given value, lines represent median values).

	Number of Metastatic Mice	Sites of Metastases
Tyr::Nras$^{Q61K/°}$; INK4a$^{-/-}$; P-Rex1$^{-/-}$	2/4	Skin (1), LN (1), Lung (1)
Tyr::Nras$^{Q61K/°}$; INK4a$^{-/-}$; P-Rex$^{+/+}$	5/5	Liver (5), kidney (5), lung (4), LN (3), Spleen (3), Peritoneal (2), Skin (2), Heart (1)

Supplementary Table S1. Endogenous P-Rex1 facilitates metastases to distant sites following the intravasation step. Table indicating number of mice with metastases as well as range of metastatic sites between BL6 mice TV-treated with either *Tyr::Nras$^{Q61K/°}$; INK4a$^{-/-}$; P-Rex$^{+/+}$* murine melanocytes or *Tyr::Nras$^{Q61K/°}$; INK4a$^{-/-}$; P-Rex1$^{-/-}$* murine melanocytes.

Cell Line	Braf status	Nras status
WM852	WT	Q61R
LU1205	V600E	WT
MeWo	WT	WT
A375M	V600E	WT
WM793	V600E	WT
WM983A	V600E	WT
WM983B	V600E	WT
WM1366	WT	Q61L
SK28	V600E	WT
SK29	V600E	WT
Rosi	WT	WT
Daju	V600E	WT
Dauv-1	V600E	WT
Mull	V600E	WT
Lyse	WT	Q61K
Gerlach	WT	Q61K
501Mel	V600E	WT
G1	WT	WT
T1	WT	WT
888mel	V600E	WT
Quar	V600E	WT
MNT-1	WT	WT
SKMEL3	V600E	WT

Supplementary Table S2. BRaf and NRas mutation status of human melanoma-derived cell lines used in RT-PCR.

	Melanoma Mets	No Melanoma Mets
High P-Rex1	4	8
Low P-Rex1	0	12
	100% sensitive (p=0.005)	**60% specific**

Supplementary Table S3. High P-Rex1 mRNA in cell lines is sensitive for detecting metastatic melanoma development in immuno-deficient mice. P-Rex1 mRNA levels divided into those above and below median value ('high' vs 'low'; chi-square test).

Cell Line	Braf status	Nras status	Growth phase
NHM	WT	WT	N/A
SK-Mel 23	WT	WT	Met
SK-Mel 187	WT	WT	VGP
CHL1	WT	WT	Met
Mel505	WT	WT	VGP
SK-Mel 2	WT	Q61R	Met
SK-Mel 119	WT	Q61R	Met
SK-Mel 147	WT	Q61R	Met
SBCL2	WT	Q61R	RGP
Mel224	WT	Q61R	Met
A375	V600E	WT	VGP
Colo 829	V600E	WT	Met
SK-Mel 5	V600E	WT	Met
WM35	V600I	WT	RGP
WM266.4	V600D	WT	VGP
WM278	V600E	WT	VGP
WM793	V600E	WT	VGP
WM902b	V600E	WT	VGP
WM1552c	V600E	WT	RGP
WM1789	K601E	WT	RGP

Supplementary Table S4. BRaf and NRas mutation status of human melanoma-derived cell lines used in Western blots. Further data on growth phase of originating tumour also. RGP = radial growth phase; Met = metastatic; NHM = normal human melanocytes.

SUPPLEMENTARY METHODS

Ex vivo melanoblast live imaging A freshly dissected E15.5 embryonic skin sample was sandwiched between a nuclepore membrane (Whatman) and a gas permeable Lumox membrane in Greiner Lumox culture dish (Greiner Bio-One GmbH) so that the epidermal side of skin was in contact with Lumox membrane. To immobilize the sample, Growth Factor Reduced Matrigel (BD Bioscience) was used to cover the whole assembly and incubated at 37°C for 10 min. Culture medium (Phenol red free DMEM supplied with 10% FBS) was added. Drugs/inhibitors were added to Matrigel and medium 1 hr before imaging. Time-lapse images were captured using an Olympus FV1000 or Nikon A1 confocal microscope in a 37°C chamber with 5% CO_2 at 20× magnification for 6h with slices every 7.5m.

RT-PCR For cell lines, total RNA was isolated from cells as above. 1ug of total RNA was reverse transcribed using the MLV RT-Enzyme (Invitrogen). Real time PCR was realized using the IQ™ SYBR® Green supermix (Biorad). P-Rex1 primers were used at 900nM (Fwd: GAA AGT GCT GGA GAA CGT GGA and Rev: TGC CCT GAG TTT GCG GTA A). Relative expression was calculated using the comparative ΔΔCt method. Briefly, this method compares the amount of target gene expression (P-Rex1) relative to an endogenous control (TBP, Fwd: CAC GAA CCA CGG CAC TGA TT Rev: TTT TCT TGC TGC CAG TCT GGA C), within a sample to normalize the expression. Within a group of samples, one appropriate sample is chosen as a calibrator sample (501mel). Each sample is then compared to the nominated reference to give the relative expression of the target gene compare to this reference sample.

For embryo skin, E14.5 (Tyr::CreB/R26YFPR) skin was dissected in PBS on ice. Subsequently skin was digested over night in 0.05% collagenase and then dissociated mechanically using a pipette. Cells were sorted by FACS into sterile PBS and RNA preps prepared using Qiagen RNAeasy plus kit. cDNA was

prepared using the Roche first strand cDNA synthesis kit. Primer sequences as follows: Prex1, Ex22_23_F, FGCACGGTGTGGTTTACGAAT; Prex1, Ex22_23_R, TCTCCAGCTTGGTGTCACAG; Prex1, Ex_37_38_F, TCTACCGCCTCATGAAGACC; Prex1, Ex_37_38_R, ATGACACACTTGGGCAACAG; Prex1, Ex1_3_F, GCCTCCGTCTGTGCGTACT; Prex1, Ex1_3_R, CAGGATGTCCTCAATGTTGG; Dct, F, TGTGCAAGATTGCCTGTCTC; Dct, R, GTTGCTCTGCGGTTAGGAAG; Tyr, F, ATGCACCTATCGGCCATAAC; Tyr, R, ATAACAGCTCCCACCAGTGC; GAPDH_F AAGGTCATCCATGACAACTTTGG; GAPDH, R, AAGAGTGGGAGTTGCTGTTGAAG.

Small Animal Regulations All studies were conducted in accordance with UK home office guidelines. All mice were maintained under non-barrier conditions and given a standard diet (Harlan) and water *ad libitum*. P-Rex1$^{-/-}$ mice were back-crossed ten times to C57BL6 backgound. Tyr::Nras$^{Q61K/°}$ and Tyr::Nras$^{Q61K/°}$; INK4a$^{-/-}$ mice were obtained from the Swiss Institute for Experimental Cancer Research (Lausanne, Switzerland). Dct-lacZ transgenic animals were obtained from the MRC Human Genetics Unit (Edinburgh, UK). All mouse experiments were performed on C57Bl6J background apart from DCT experiments which were performed on mice which 50% ICR and 50% C57BL6J.